Power System Technology
ISSN:1000-3673

Received: 16-02-2026 *Revised: 20-03-2026* *Accepted: 10-04-2026*

Influence of Vent Aperture Size on Natural Convection Cooling of Pv Panels in a Bipv Double-Skin Façade

Mohammed-Abdellatif Bensaci[1], Aissa Abidi-Saad[1] , Djamel Belatrache[2], Abdelkader Harrouz[3]

[1]Laboratory of Petroleum, Gas and Aquifer Underground Reservoirs, Kasdi Merbah University, Ouargla 30000, Algeria

[2] VPRS Laboratory, Kasdi Merbah University, 30000 Ouargla, Algeria

[3] Department of Electrical Engineering, Ahmed Draïa University, Adrar, Algeria

Abstrect

double-skin façades (DSF) by enhancing heat dissipation from the rear surface of the PV module. A numerical investigation is conducted to analyze heat removal driven by natural convection within the DSF air channel. The system includes a vent aperture located on the unheated façade to facilitate airflow circulation. The double-skin channel is subjected to non-uniform heating with a uniform heat flux and is immersed in a water-filled reservoir to reproduce environmental conditions and generate overpressure at the inlet and outlet of the PV-DSF channel. A two-dimensional steady laminar flow model is solved using the finite volume method under realistic geometric and boundary conditions. The study examines the influence of the vent aperture on the heat transfer characteristics and flow behavior within the channel. Numerical results are presented in terms of Nusselt number, temperature distribution, isotherms, and velocity profiles. The numerical predictions are validated against experimental data, showing very good agreement.

Key words: Free convection; Uneven heating; Vent aperture; BIPV double-skin façade.

1. Introduction

Several works in the literature present PV panels modeled by a vertical or inclined unevenly heated channel [1-3], in order to understand or improve the flow and heat transfer in such systems. The vertical position corresponds to the situation where the PV modules are integrated in buildings as Double Skin Facades (DSFs). PV panels constitute a renewable source of electric energy, yet the fraction of solar energy actually converted by PV panels into electricity is only about 18–20% [4], due to an internal temperature rise, which is responsible for a decrease in both electrical conversion efficiency and reliability. PV panels can be used in the building industry due to the large surface offered by the building envelope (known as Building Integrated Photovoltaics, or BIPV). The integration of PV panels in building envelopes is an effective means of collecting solar energy and may be implemented in the field of “hybrid”

Power System Technology
ISSN:1000-3673
Received: 16-02-2026 Revised: 20-03-2026 Accepted: 10-04-2026

applications like PV/T (Photovoltaic/Thermal) solar collectors, where the electricity produced by PV panels can be used for both the heating and cooling needs of the building. Many techniques exist to control and improve the heat transfer and fluid flow within such systems. Using free convection to remove heat from the backside of a PV panel has many benefits: such a thermally-driven flow is economic, dependable, noiseless and maintenance free. Furthermore, it provides flow rates comparable to those obtained with forced ventilation in channels, as indicated by Brinkworth et al. [5].

The control and limitation of the operating temperatures experienced in PV panels are the main challenges in the utilization of building integrated photovoltaic systems. Passive cooling of the PV panels by natural convection is ensured by air circulation within the narrow channel between the PV array and the building, as noted by Sandberg and Moshfegh [6]. Mittelman et al. [7] performed a scale analysis as well as a numerical study on tilted PV modules with a back mounted air channel. In their study, various parameters are considered: a modified Rayleigh number ranging from 102 to 108, aspect ratios between 15 and 50 and tilt angles between 30° and 90°. A generalized correlation for the average Nusselt number for the combined convective–radiative cooling is developed. Results indicate that the temperature of the PV panels decreases by as much as 10–20 K due to the sole presence of the channel behind them, resulting in an absolute efficiency gain of 1–2%. Numerous experimental and numerical works on natural convection inside vertical channels constructed by DSFs have been carried out [8-19]. Many geometric modifications have been applied to DSF with the purpose of enhancing and controlling both flow and heat transfer, aimed at cooling PV panels. Abidi-Saad et al. [20] and [21] have carried out experimental and numerical investigations respectively, using water as solar fluid. The authors concentrated on the effect of the size and position of two symmetrically attached ribs inside an unevenly heated channel, representative of PV panels integrated in a double-skin facade. In the numerical work, an optimal ribs size is found, which maximizes heat transfer and mass flow rate as well. The authors highlighted that the later findings are suitable for hybrid solar applications (PV/T solar collectors). Besides, in the experimental study, the optimal position of the two ribs in terms of heat transfer enhancement is located at the top of the heated zone. It is also worth noting that both works highlight a reversed flow. Some works mention internal heated or adiabatic plates and baffles in the air gap [22-27], while others increase heat transfer and extraction using the chimney effect downstream of the DSF-channel [28-31]. Kimouche et al. [32] performed numerical investigation about the effect of the inclination of the adiabatic facade of unevenly heated channel on convective heat transfer and water flow. Their study was conducted for the same geometry studied here, but without vent aperture, under various tilt angels of the adiabatic facade ($-10° \leq \alpha \leq +10°$) and for a modified Rayleigh number $Ra^* = 4.5 \times 10^6$. However, the literature is relatively sparse as to the effects of a vent aperture on the enhancement of heat

Power System Technology
ISSN:1000-3673
Received: 16-02-2026 Revised: 20-03-2026 Accepted: 10-04-2026

removal from the back side of the PV panel. Azevedo and Sparrow [33] evaluated the effect of size and position of vent aperture on water natural convection flow and heat transfer inside one-sided heated vertical channel. Their calculation domain was restricted to the channel only, which has one wall entirely heated with uniform temperature while the opposite vented-wall is adiabatic. They revealed that the channel average Nusselt number remained unaltered by the variation of size and location of the vent opening. Bouraoui et al. [34] have investigated the effect of a vent aperture in the adiabatic facade of a DSF. The authors focused on the dynamic effects stemming from a change in the size and position of the vent aperture. In fact, such problem can be numerically modeled in two ways, (i) simulating the whole domain: the PVDSF-channel and its environment or (ii) simulating only the PVDSF-channel restricted to its borders. The second way is intricate in that the boundary conditions are theoretically unknown at low and high channel interfaces because the main flow belongs to the computation domain too, as detailed in Refs. [35, 36]. The present study has been carried out, for the whole domain (PVDSF-channel and its environment), to assess the influence of the size of a vent aperture on both heat transfer and flow dynamics. It focuses more specifically on thermal aspects, in order to reduce the temperature of PV panels integrated in DSFs to enhance their energy performance. Since the PV-DSFs were modelled by a vertical/inclined unevenly heated channel, the current prototype, consisting in a vertical plane channel, was immersed in a water-filled reservoir acting as the environment. The use of water as working fluid aims at minimizing the thermal radiation effect. Furthermore, water-based PV/T collector systems seem more attractive and efficient than air-based systems in hot and humid climate [16]. As a matter of fact, Daghigh et al. [37] have highlighted the significance and difficulty of cooling a PV cell in an attempt to enhance the efficiency of a PV/T system under these climate conditions. Abdullah et al. [38], in their recent work, highlighted that the highest efficiency of PV/Trombe wall is found when using water as cooling fluid. Also, Himanshu et al. [39] improved the performance of inclined rooftop solar chimney by 10% using humid air compared to that of dry air. Moreover, immersing the DSF-channel in a water reservoir allows us to get over pressure boundary conditions in the inlet and outlet of the DSF-channel. In fact, these conditions are likely to complicate the study in the case of natural convection and if the DSF-channel is the only domain of study. The experiment is conducted in realistic environmental and geometric conditions. For instance, the heat flux density used corresponds to the average environmental conditions of insolation in France, and the DSF-channel features an aspect ratio of Rf = 5.2, within the range of those found in the literature for horizontally divided DSFs of tall buildings [10].

Power System Technology
ISSN:1000-3673
Received: 16-02-2026 Revised: 20-03-2026 Accepted: 10-04-2026

2. DSF-channel features

The physical problem considered here is natural convection in an unevenly heated channel, forming a prototype of PV-DSF, with two parallel vertical facades 376 mm high. The two facades are spaced by a gap 'S' of 36 mm. The left facade has a heated central zone (corresponding to a PV panel of height H = 188 mm) encompassed by two adiabatic extensions (length H/2) at its both ends. The aspect ratio of the DSF-channel (H/S) is equal to 5.2. The opposite facade is totally unheated. This facade has a vent aperture of different sizes (S/3, 2S/3, S and 4S/3), and is aligned with the base of the heated area of the heated facade (see Fig. 1). In addition, the DSF-channel has in its bottom-end a quarter circle of radius equal to 36 mm to steer better the flow conditions at the DSF-channel inlet. The DSF-channel is immersed in a vertical top-open reservoir. This later is made of Plexiglas® plates of 20 mm thickness and filled with water. The square base plate is of 0.5 m side and the other four standing plates are of 1 m height (see Fig. 1).

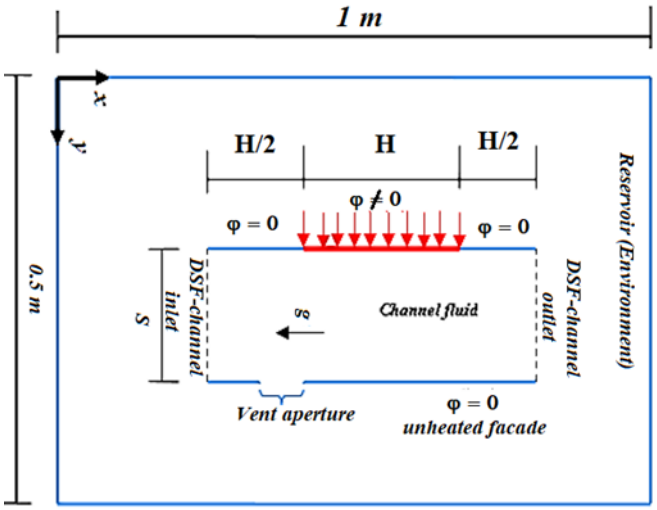

Fig. 1 PV-DSF channel and its environment

3. Methodology description

To model the flow motion and heat transfer within the studied domain (the DSF-channel and its environment), the governing equations Eqs. (1-4) are employed, which are the mass transport (1), momentum (2), (3), and energy (4) equations. The motion of the Newtonian incompressible fluid is assumed to be unsteady, laminar, and 2D.

$$\frac{\partial \rho}{\partial t} + \frac{\partial \rho u}{\partial x} + \frac{\partial \rho v}{\partial y} = 0 \quad (1)$$

Power System Technology
ISSN:1000-3673

Received: 16-02-2026 Revised: 20-03-2026 Accepted: 10-04-2026

$$\left(\frac{\partial u}{\partial t}+\rho u\frac{\partial u}{\partial x}+\rho v\frac{\partial u}{\partial y}\right)=-\frac{\partial P^{*}}{\partial x}+\frac{\partial}{\partial x}\left(\mu\frac{\partial u}{\partial x}\right)+\frac{\partial}{\partial y}\left(\mu\frac{\partial u}{\partial y}\right)+\frac{\partial u}{\partial x}\frac{\partial \mu}{\partial x}+\frac{\partial v}{\partial x}\frac{\partial \mu}{\partial y} \quad (2)$$

$$\left(\frac{\partial v}{\partial t}+\rho u\frac{\partial v}{\partial x}+\rho v\frac{\partial v}{\partial y}\right)=-\frac{\partial P^{*}}{\partial y}+\frac{\partial}{\partial x}\left(\mu\frac{\partial v}{\partial x}\right)+\frac{\partial}{\partial y}\left(\mu\frac{\partial v}{\partial y}\right)+\frac{\partial u}{\partial y}\frac{\partial \mu}{\partial x}+\frac{\partial v}{\partial y}\frac{\partial \mu}{\partial y}-\rho g \quad (3)$$

$$\rho C_p\left(\frac{\partial \theta}{\partial t}+u\frac{\partial \theta}{\partial x}+v\frac{\partial \theta}{\partial y}\right)=\frac{\partial}{\partial x}\left(k\frac{\partial \theta}{\partial x}\right)+\frac{\partial}{\partial y}\left(k\frac{\partial \theta}{\partial y}\right) \quad (4)$$

The physical properties of the employed fluid are chosen to be temperature dependent to fit the reality. To this end polynomial temperature dependent formulae [40, 41] are used and given as follows:

Density: $\rho(\theta)=5.3738\times10^{-10}\times\theta^{5}-9.59976\times10^{-7}\times\theta^{4}+6.93809\times10^{-4}\times\theta^{3}-0.255822\times\theta^{2}+47.8074\times\theta-2584.53$ (5)

Thermal conductivity: $k(\theta)=5.15307\times10^{-11}\times\theta^{5}-8.15212\times10^{-8}\times\theta^{4}+5.138\times10^{-5}\times\theta^{3}-1.61344\times10^{-2}\times\theta^{2}+2.52691\times\theta-157.532$ (6)

Specific heat: $C_p(\theta)=-4.51782\times10^{-8}\times\theta^{5}+7.61613\times10^{-5}\times\theta^{4}-5.12699\times10^{-2}\times\theta^{3}+17.2363\times\theta^{2}-2894.85\times\theta+198532$ (7)

Dynamic viscosity: $\mu(\theta)=-4.37087\times10^{-13}\times\theta^{5}+7.38482\times10^{-10}\times\theta^{4}-4.99292\times10^{-7}\times\theta^{3}+1.68946\times10^{-4}\times\theta^{2}-2.86313\times10^{-2}\times\theta+1.94641$ (8)

The above-mentioned 2D governing equations were solved using ANSYS Fluent CFD code. This later uses finite volume method for the transport equations discretization which they were successively solved using pressure-based solver. To solve concurrently the mass transport and momentum equations, the Coupled algorithm is employed which ensure the velocity-pressure coupling and offers strong dynamic-thermal fields interdependency. The schemes Second-Order Implicit, Second-Order Upwind and Central Difference were used for discretizing the time derivative, convective, and diffusive terms respectively. The grid independence study has been performed to ensure that the solution is independent on the mesh size and to find out the appropriate grid size for the computation with respect to the time and accuracy of results. To this end, five grid experiments within the DSF-channel were conducted, namely: 25000, 27000, 28000, 30000 and 33000 elements respectively. It is found that the grid size of 27000 elements inside the channel (42072 elements in the whole domain) is adequate to provide

Power System Technology
ISSN:1000-3673
Received: 16-02-2026 Revised: 20-03-2026 Accepted: 10-04-2026

satisfactory accuracy of the results. The grid experiments were carried out for a vent aperture size equal to 2S/3 and a modified Rayleigh number Ra* equal to 4.5×10^6. The convergence criteria were based on the absolute residuals resulting from the integration of the conservation equations over finite control volumes. For all simulations performed in this study, convergence was considered achieved as soon as residuals decrease below a threshold of 10-4 for all governing equations.

4. Results

Prior to any numerical study, it is necessary to check the reliability of the developed numerical model. To do so, numerical results are compared with experimental data found by Ospir et al. [11] using the laser tomography technique. In this experiment, Rilsan quasi-spherical particles (tracers) of average diameter 100 μm and density ρ=1060 kg/m^3 (close to that of water) were used. A comparison between the streamlines obtained experimentally and through numerical simulation is made, as illustrated in Fig 2. The validation is performed on a PV-DSF channel without vent aperture on the unheated facade, for a modified Rayleigh number of 4.5×10^6 (= 510 W/m²) and at t = 30 min, which was found to be a sufficient time to reach a steady-state flow inside the channel [11]. From Fig 2, it can be noted that both dynamic flow structures are very similar; namely composed by a boundary layer upward flow near the heated facade and a recirculation zone at the channel outlet adjacent to the unheated facade. Very good agreement is also observed between the numerical and experimental recirculation sizes.

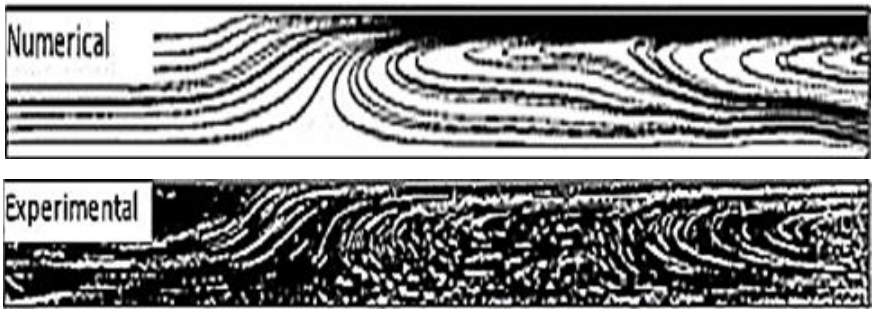

Fig. 2 Validation between experimental and simulation results for Ra* = 4.5×10^6.

In order to make the model even more trustworthy, a comparison of the thermal field with experimental data gathered by Polidori et al. [12] is performed. Validation is carried out between our numerical temperature differences along the heated zone (corresponding to the back of the PV panels) and those found experimentally for = 445 W/m², as seen in Fig. 3. The purpose of the experimental study presented in [12] was to measure the heat flux delivered to the fluid. To this end, the authors measured the temperature along the median axis of the heated zone and compared it to a classical theoretical model of free convection boundary layer flow past a semi-infinite heated plate. This configuration can actually be realized by removing

Power System Technology
ISSN:1000-3673
Received: 16-02-2026 Revised: 20-03-2026 Accepted: 10-04-2026

the unheated facade from the considered channel, in an attempt to avoid heat flux misevaluation and bias owing to probable recirculation flow structures in the channel. The same configuration is considered here. As seen in Fig. 3, very good concordance is found between the two results in terms of temperature difference.

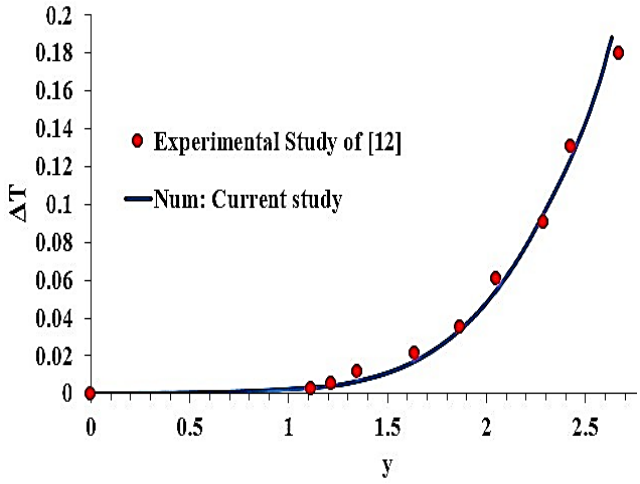

Fig. 3 Validation between experimental temperature difference and current numerical results for □ = 445 W/m².

4.1. The vent aperture size effect on velocity profiles at different heights of the DSF-channel

The effect of the vent aperture sizes (S/3, 2S/3, S and 4S/3) on vertical velocity profiles at different heights of the channel may be assessed directly from the results depicted in Figs. 4a-d, i.e., at the channel entrance, heated zone base, center of the heated zone, heated zone head, and DSF-channel exit (y = 0, y = H/2, y = H, y = 3H/2, and y = 2H). The X-axis in Figs. 4a-d is dimensionless via the formula X=x/S. It clearly appears in Figures (4a-d) that the vertical velocity variations are similar for the various vent aperture sizes. The velocity profile is almost fully developed until the base of the PV panel (the heated zone) and evolves in a boundary layer type beyond. A remarkable characteristic is the high acceleration in the vicinity of the rear of the PV panels, followed by a decrease with even negative velocities due to the return flow. The minimum values for the velocities are reached for small heights (y=0, y = H/2) and the maximum values are found for heights equals to (y = H, y = 3H/2, and y = 2H). Furthermore, the maximum magnitude of the axial velocity is reached for the large vent aperture size (Fig. 4d).

Power System Technology
ISSN:1000-3673
Received: 16-02-2026 Revised: 20-03-2026 Accepted: 10-04-2026

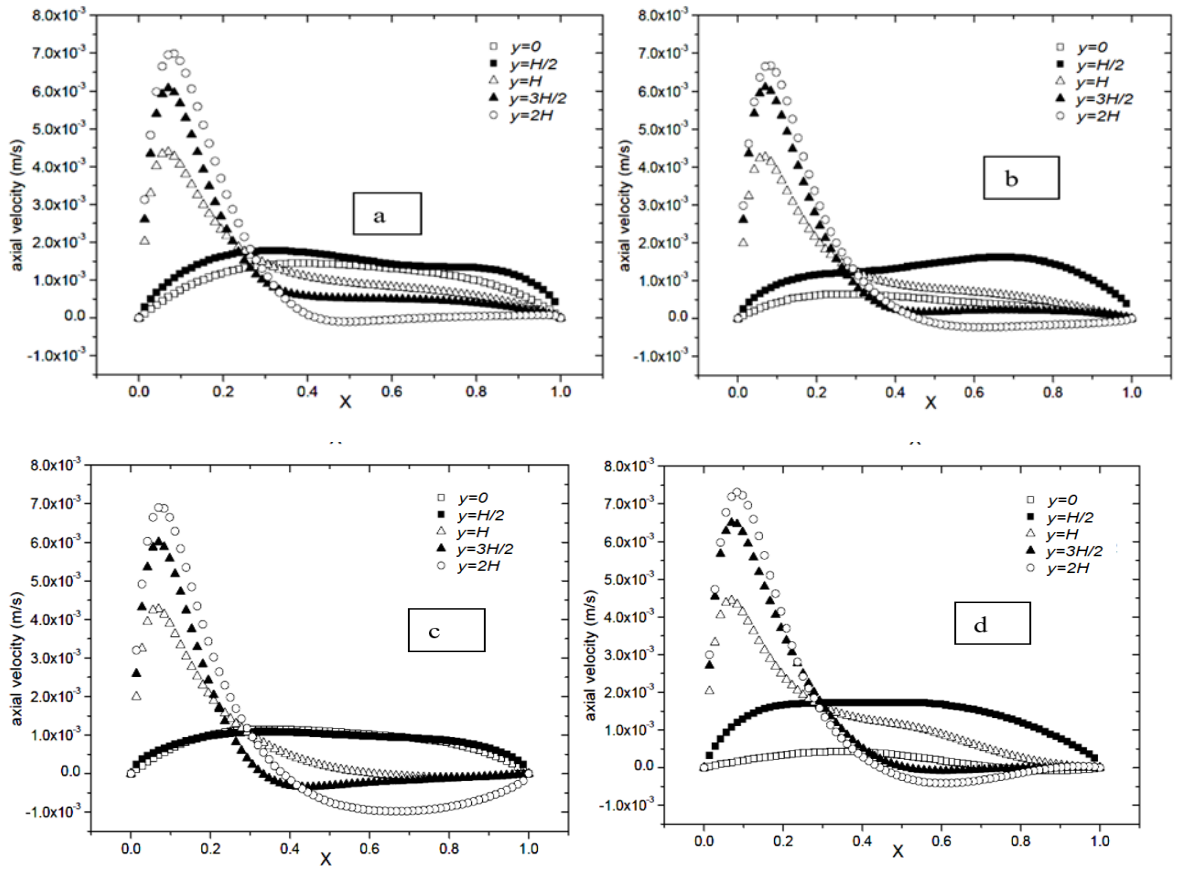

Fig.4 Axial velocity profiles at different heights of the PV-DSF channel for various vent aperture sizes (a) S/3, (b) 2S/3, (c) S (d) 4S/3 for Ra* = 4.5×10⁶.

4.2. The vent aperture size effect on temperature fields

The variation between temperature at t = 30 min (laminar regime) and initial temperature T0 is shown in Fig 5. The curves are plotted at a vertical line x = 0.4 m (between the DSF-channel adiabatic facade and the right facade of the reservoir). From these curves, it may be concluded that larger vent aperture sizes result in greater temperature differences inside the reservoir (environment), with a maximum of 0.6 K for the largest vent aperture of 4S/3. Fig 6 shows temperature distribution along the entire PV facade (rear of the PV panels, upstream and downstream adiabatic extensions). One can see the same pattern of the temperature profiles for all vent aperture sizes. At the PV-DSF channel entry, along the downstream adiabatic extension, there is no heat transfer where the temperature is the same as the ambient. Beyond that, along the rear of the PV panels, the temperature increases progressively until it arrives at its maximum amount at the end of the rear of PV panels, revealing considerable heat transfer. At the PV-DSF channel way-out, along the upstream adiabatic extension, the temperature

Power System Technology
ISSN:1000-3673
Received: 16-02-2026 Revised: 20-03-2026 Accepted: 10-04-2026

diminishes sharply. The important finding is that the temperature at the rear of the PV panel for the vent aperture size "2S/3" is the smallest which indicates the occurrence of the largest heat transfer. Whereas, the temperature evolution for the vent aperture size "4S/3" is the largest which means the smallest heat transfer was happened for this size. These findings are confirmed by isotherms distribution depicted in Fig 7 (next section).

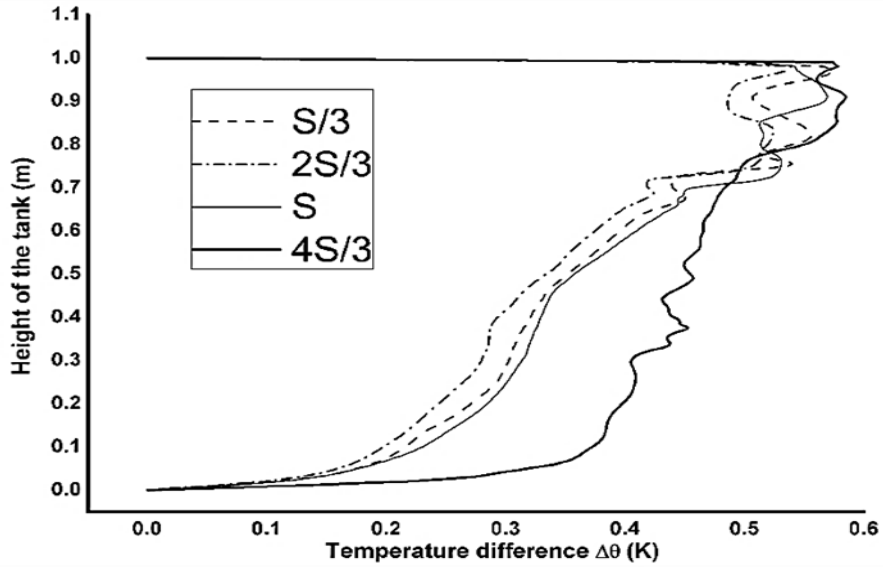

Fig.5 Vertical profile of temperature difference for various vent aperture sizes and for Ra* = 4.5×10^6.

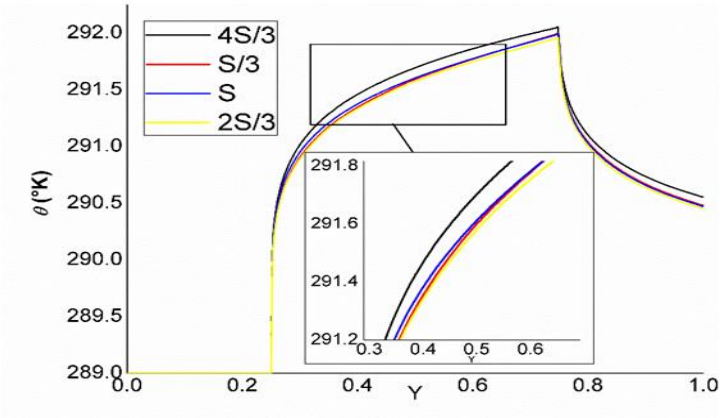

Fig. 6. Temperature distribution along the PV facade for various vent aperture sizes in the PV- DSF channel for Ra* = 4.5×10^6.

Power System Technology
ISSN:1000-3673
Received: 16-02-2026 Revised: 20-03-2026 Accepted: 10-04-2026

The temperature field within the PV-DSF channel as well as the whole computation domain (DSF-channel and its environment) are depicted in Fig. 7. Quite interestingly, the presence of a vent aperture at the base of the unheated facade has no effect on the thermal boundary layer (see Fig 7a), which constitutes the flow source. The analysis of Fig. 6 also underlines that for a vent aperture size smaller than the DSF-channel width "S" (i.e., S/3 and 2S/3), a significant amount of cold fluid is retained inside the DSF-channel. It almost covers the whole heated zone (PV panel) for vent aperture size equal to 2S/3. By contrast, larger DSF-channel widths lead to hotter fluid within the DSF-channel and its environment (see Fig 7). This finding may arise from the fact that when the size of the vent aperture is large enough, the fluid entering through the DSF-channel inlet is almost superseded by that flowing through the large vent aperture. Besides, the large vent aperture pumps the hot fluid out of the upper part of the reservoir (hot fluid), not from below (cold fluid), which results in the hot fluid being heated.

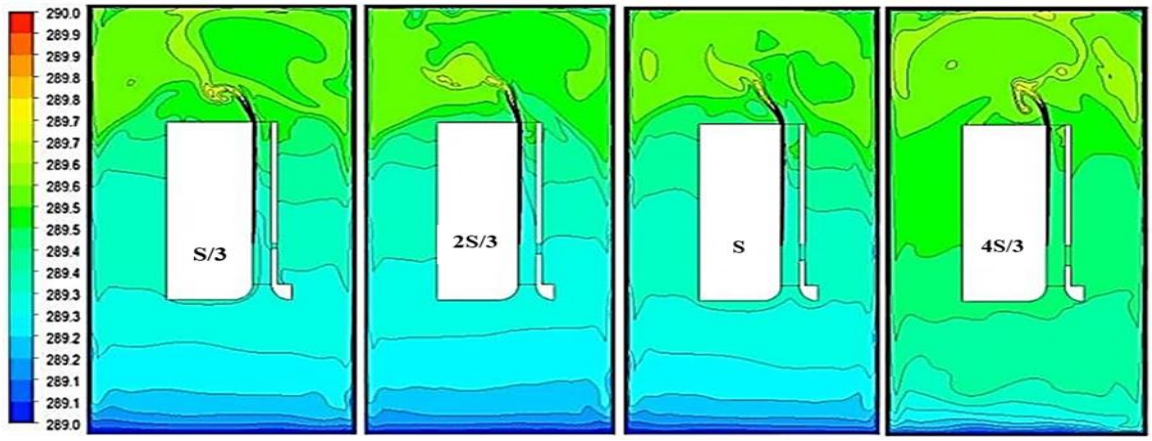

Fig. 7. Isotherms plots for various vent aperture sizes in the PV- DSF channel and its environment (the reservoir), for Ra* = 4.5×10^6.

4.3. The vent aperture size effect on heat transfer

The heat transfer is characterized by the average Nusselt number which may be calculated using the following equation:

$$Nu_{ave} = \frac{h_{ave} \times H}{k} \quad (9)$$

$$h_{ave} = \frac{1}{H}\int_{H/2}^{3H/2} \frac{\varphi}{(\theta_w - \theta_0)} dy \quad (10)$$

Power System Technology
ISSN:1000-3673
Received: 16-02-2026 Revised: 20-03-2026 Accepted: 10-04-2026

Figure 8 represents the evolution of the average Nusselt number along the heated zone (PV panel). As seen in this figure, heat transfer is enhanced for vent aperture sizes smaller than the DSF channel width, with a maximum value found for vent aperture size of 2S/3. As mentioned earlier, this vent aperture size makes it possible for a significant quantity of cold fluid to flow through the DSF channel and thus almost cover the whole heated zone (rear of the PV panel). Heat dissipation at the back side of the PV panel is therefore optimal.

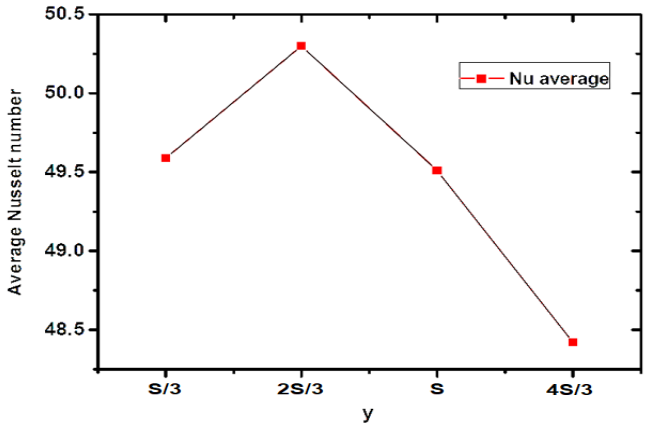

Fig. 8 Average Nusselt number along the heated facade (rear of the PV panel) for various vent aperture sizes and for Ra* = 4. 5×10^6.

5. Conclusion

The energy efficiency of PV panels is limited by their inherent temperature increase. Not surprisingly, reducing their heating has positive consequences in their electricity production. Any heat transfer enhancement should thus be considered, especially when stemming from free, cheap and simple techniques. In this study, the effect of vent aperture on heat transfer enhancement in a PV-DSF channel is investigated using numerical tools, with the purpose of cooling down the PV panel integrated in the building. The study is performed for Ra* = 4.5.10^6 with a PV-DSF-channel aspect ratio of 5.2 and for four sizes of the vent aperture at the base of the PVDSF-channel. It is reminded that the selected value of aspect ratios lies within the range of those found for horizontally divided double-skin facades of tall buildings [10]. Overall, the thermal fields are strongly affected by the vent aperture size and based on the results presented herein, several conclusions may be drawn. First, a large vent aperture at the base of the PVDSF-channel affects the thermal field within it as well as the reservoir (environment). Then, a vent aperture narrower than the PV-DSF width is suitable for cooling purposes of the PV panel within a PVDSF. Conversely, a vent aperture of size larger than the PV-DSF width is adequate if one aims at heating the building. Finally, an increase in the vent aperture size has no effect of the thermal boundary layer and profiles of axial velocities, at least for the studied vertical

Power System Technology
ISSN:1000-3673

Received: 16-02-2026 *Revised: 20-03-2026* *Accepted: 10-04-2026*

positions. It is also worth noting that a maximal heat dissipation at the back of the PV panel is achieved with a vent aperture size of 2S/3.

References

[1] Gan G (1998) A parametric study of Trombe walls for passive cooling of buildings. Energy Build 27: 37–43. https://doi.org/10.1016/S0378-7788(97)00024-8

[2] Lau GE, Sanvicente E, Yeoh GH, Timchenko V, Fossa M, Ménézo, Giroux-Julie CS (2012) Modelling of natural convection in vertical and tilted photovoltaic applications. Energy Build 55: 810–822. https://doi.org/10.1016/j.enbuild.2012.10.014

[3] Christian S, Patrice J, José LM, Francisco SJ (2011) Heat transfer and mass flow correlations for ventilated facades. Energy Build 43: 3696–3703. https://doi.org/10.1016/j.enbuild.2011.10.002

[4] Candanedo LM, Athienitis A, Park K (2011) Convective heat transfer coefficients in a building-integrated photovoltaic/thermal system, Journal of Solar Energy Engineering 133: 021002-1–021002- 14. https://doi.org/10.1115/1.4003145

[5] Brinkworth BJ, Cross BM, Marshall RH, Yang H (1997) Thermal regulation of photovoltaic cladding, Sol. Energy 61: 169-178. https://doi.org/10.1016/S0038-092X(97)00044-3

[6] Sandberg M, Moshfegh B (2002) Buoyancy-induced air flow in photovoltaic facades: effect of geometry of the air gap and location of solar cell modules, Build. Environ 37: 211-218. https://doi.org/10.1016/S0360-1323(01)00025-7

[7] Mittelman G, Alshare A, Davidson J.H (2009) A model and heat transfer correlation for rooftop integrated photovoltaics with a passive air-cooling channel. Sol. Energy 83: 1150–1160. https://doi.org/10.1016/j.solener.2009.01.015

[8] Elenbaas W (1942) Heat dissipation of parallel plates by free convection. Physica 9:1–28. https://doi.org/10.1016/S0031-8914(42)90053-3

[9] Webb B.W, Hill D.P (1989) High Rayleigh number laminar natural convection in an unevenly heated vertical channel, J. Heat Transfer 111 (3): 649–656. DOI:10.1115/1.3250732

[10] Popa C, Ospir D, Fohanno S, Chereches NC (2012) Numerical simulation of dynamical aspects of natural convection flow in a double-skin façade. Energy Build 50: 229–233.

[11] Ospir D, Popa C, Chereches C, Polidori G, Fohanno S (2012) Flow visualization of natural convection in a vertical channel with asymmetric heating. Int, Commun Heat Mass Transf;39:486– 493 https://doi.org/10.1016/j.icheatmasstransfer.2012.02.005

Power System Technology
ISSN:1000-3673

Received: 16-02-2026 *Revised: 20-03-2026* *Accepted: 10-04-2026*

[12] Polidori G, Fatnassi S, Ben Maad R, Fohanno S, Beaumont F (2015) Early- stage dynamics in the onset of free-convective reversal flow in an open-ended channel unevenly heated. Int J Therm Sci 88: 40–46. 10.1016/j.ijthermalsci.2014.09.011

[13] Fatnassi S, Ben-Maad R, Abidi-Saad A, Polidori G (2017) On the appearance of natural convection induced reversed flow: Precocious hydrodynamic experimental study; Application to PV- DSF systems, Applied Thermal Engineering 127 1598–1607.

[14] Yilmaz, T., Gilchrist, A (2007) Temperature and velocity field characteristics of turbulent natural convection in a vertical parallel- plate channel with asymmetric heating. Heat Mass Transf 43, 707–719. https://doi.org/10.1007/s00231-007-0234-y

[15] Dupont F, Ternat F, Samot S, Blonbou R (2013) Two-dimension experimental study of the reverse flow in a free convection channel with active walls differentially heated. Exp. Therm. Fluid Sci 47: 150–157. https://doi.org/10.1016/j.expthermflusci.2013.01.010

[16] Hemmer C, Abidi-Saad A, Popa CV, Polidori G (2017) Early development of unsteady convective laminar flow in an inclined channel using CFD: Application to PV panels. Solar Energy146: 221–229. https://doi.org/10.1016/j.solener.2017.02.050

[17] Kimouche N, Mahri Z, Abidi-Saad A, Popa C, Polidori G, Maalouf C (2017) Effect of inclination angle of the adiabatic wall in unevenly heated channel on natural convection: Application to double-skin façade design, Journal of Building Engineering12:171–177. DOI:10.1007/s00231-016-1853-y

[18] Yassine Cherif, Emilio Sassine, Stephane Lassue, Laurent Zalewski (2020) Experimental and numerical natural convection in an asymmetrically heated double vertical facade, International Journal of Thermal Sciences, Vol 152, 106288. https://doi.org/10.1016/j.ijthermalsci.2020.106288

[19] Cristina Sotelo-Salas, Carlos Escobar-del Pozo, Carlos J. Esparza-López (2021) Thermal assessment of spray evaporative cooling in opaque double skin facade for cooling load reduction in hot arid climate, Journal of Building Engineering, Vol 38, 102156. https://doi.org/10.1016/j.jobe.2021.102156

[20] Abidi-Saad A, Kadja M, Popa C, Polidori G (2017) Effect of adiabatic square ribs on natural convection in an unevenly heated channel, Heat Mass Transfer 53(2): 743-752. DOI:10.1007/s00231-016-1853-y

[21] Abidi-Saad A, Polidori G, Kadja M, Beaumont F, Popa CV, Korichi A (2016) Experimental investigation of natural convection in a vertical rib-roughened channel with asymmetric heating, Mechanics Research Communications76: 1–10. https://doi.org/10.1016/j.mechrescom.2016.06.001

Power System Technology
ISSN:1000-3673

Received: 16-02-2026 *Revised: 20-03-2026* *Accepted: 10-04-2026*

[22] Aihara T (1996) Augmentation of free convection heat transfer between vertical parallel plates by inserting an auxiliary plate. In: Proceedings of the 2nd European Thermal Sciences Conference, Rome, Italy

[23] Andreozzi A, Manca O (2001) Thermal and fluid dynamic behavior of symmetrically heated vertical channels with auxiliary plate. Int J Heat Fluid Flow 22: 424–432. https://doi.org/10.1016/S0142-727X(01)00080-7

[24] Andreozzi A, Manca O, Naso V (2002) Natural convection in vertical channels with an auxiliary plate. Int J Numer Methods Heat Fluid Flow 12(6):716–734. https://doi.org/10.1108/09615530210438364

[25] Taieb S, Laatar AH, Balti J (2013) Natural convection in an unevenly heated vertical channel with an adiabatic auxiliary plate. Int J Therm Sci 74: 24–36. https://doi.org/10.1016/j.ijthermalsci.2013.06.010

[26] Razavi, S.E., Adibi, T. & Faramarzi, S (2020) Impact of inclined and perforated baffles on the laminar thermo-flow behavior in rectangular channels. SN Appl. Sci. 2, 284. https://doi.org/10.1007/s42452-020-2078-8

[27] Faramarzi, S., Ghasemiasl, R. & Ghadami, F (2021) Numerical investigation of the impact of inclined baffles and an elastic vibrating beam on the thermo-fluid behavior in a rectangular channel. SN Appl. Sci. 3, 578. https://doi.org/10.1007/s42452-021-04568-7

[28] Manca O, Musto M, Naso V (2003) Experimental analysis of asymmetrical isoflux channel-chimney systems. Int J Therm Sci 42: 837– 846. https://doi.org/10.1016/S1290-0729(03)00056-5

[29] Manca O, Musto M, Naso V (2005) Experimental investigation of natural convection in an unevenly heated vertical channel with an asymmetric chimney. ASME J Heat Transf 127: 888–896. https://doi.org/10.1115/1.1928909

[30] Nasri Z, Laatar AH, Balti J (2015) Natural convection enhancement in an unevenly heated channel-chimney system. Int J Therm Sci 90:122–134. https://doi.org/10.1016/j.ijthermalsci.2014.11.033

[31] Alami AH, Ramadan M, Abdelkareem MA, Alghawi JJ, Alhattawi NT, Mohamad H A, Olabi A, (2022) Novel and practical photovoltaic applications, Thermal Science and Engineering Progress, Volume 29, 101208, https://doi.org/10.1016/j.tsep.2022.101208.

[32] Kimouche N, Mahri Z, Abidi-Saad A, Popa CV, Polidori G, Maalouf C (2017) Effect of inclination angle of the adiabatic wall in asymmetrically heated channel on natural convection: Application to double-skin façade design, Journal of Building Engineering 12: 171-177.

Power System Technology
ISSN:1000-3673

Received: 16-02-2026 *Revised: 20-03-2026* *Accepted: 10-04-2026*

[33] Azevedo LF, Sparrow EM (1986) Natural Convection in a Vertical Channel Vented to the Ambient Through an Aperture in the Channel Wall, International Journal of Heat and Mass Transfer 29: 819–830. https://doi.org/10.1016/0017-9310(86)90178-X

[34] Bouraoui M, Rouabah MS, Abidi-Saad A, Korichi A, Popa C, Polidori G (2017) Numerical simulation of a double skin with secondary ventilation flow on adiabatic wall, Frontiers in Heat and Mass Transfer (FHMT), 8: 18. DOI:10.5098/hmt.8.18

[35] Desrayaud G., Chénier E, Joulin A et al. (2013) Benchmark solutions for natural convection flows in vertical channels submitted to different open boundary conditions. Int. J. Therm. Sci, 72: 18–33. https://doi.org/10.1016/j.ijthermalsci.2013.05.003

[36] Garnier C (2014) Modélisation numérique des écoulements ouverts de convection naturelle au sein d'un canal vertical asymétriquement chauffé PhD These. University of Pierre et Marie Curie, France.

[37] Daghigh R, Ruslan MH, Sopian K (2011) Advances in liquid based photovoltaic/thermal (PV/T) collectors. Renew. Sustain. Energy Rev15: 4156–4170. https://doi.org/10.1016/j.rser.2011.07.028

[38] Abdullah A. Abdullah, Faris S. Attulla, Omer K. Ahmed, Sameer Algburi, (2022) Effect of cooling method on the performance of PV/Trombe wall: Experimental assessment, Thermal Science and Engineering Progress, Volume 30, 101273, https://doi.org/10.1016/j.tsep.

[39] Himanshu Dahire, Srinivasa Ramanujam Kannan, Sunil Kumar Saw, (2022) Effect of humidity on the performance of rooftop solar chimney, Thermal Science and Engineering Progress, Volume 27, 101026, https://doi.org/10.1016/j.tsep.

[40] Gray DD, Giorgini A (1976) The validity of the Boussinesq approximation for liquids and gases. Int J Heat Mass Transf 19: 545–551. https://doi.org/10.1016/0017-9310(76)90168-X

[41] Bejan A (1984) Convection heat transfer. Wiley-Interscience, New York Nazeer,W. A., et al., In-situ Species, Temperature and Velocity Measurements in a Pulverized Coal Flame, Combustion Sciences and Technology, 143 (1999), 2, pp. 63-77